

# Modelling of Autocatalytic Heterogeneous Dissolution Reactions. Application to Uranium Dioxide Dissolution

Sophie Lalleman<sup>a\*</sup>, Florence Charlier<sup>a</sup>, Philippe Marc<sup>a</sup>, Alastair Magnaldo<sup>a</sup>, Gilles Borda<sup>a</sup>, Eric Schaeer<sup>b</sup>

<sup>a</sup>CEA, Nuclear Energy Division, Research Department of Mining and Fuel Recycling Processes, 30207 Bagnols sur Cèze, France

<sup>b</sup>Laboratoire Réaction et Génie des Procédés, UMR 7274, CNRS – Université de Lorraine, 1 rue Grandville, BP 20451, 54001 NANCY Cedex, France  
[sophie.lalleman@cea.fr](mailto:sophie.lalleman@cea.fr)

This study deals with the modelling of uranium dioxide dissolution in nitric medium, which is a key step at the head-end of nuclear fuel reprocessing. This particular dissolution is triphasic (involving solid uranium dioxide, liquid nitric acid and gaseous nitrogen oxide products), and autocatalytic (accelerated by an unidentified reaction product), so that numerous coupled phenomena must be taken into account for a better understanding, modelling and optimization of dissolution reactors. The kinetic parameters were determined for both the catalyzed and non-catalyzed reactions. The kinetic study was realized thanks to a single particle approach and the reaction rates were measured by optical microscopy, thanks to a specific lab-scale device which ensures the absence of any external limitation. Gas-liquid exchanges were shown to have a great impact on the catalyst concentration in the reactor, and evidence of a volume reaction between the dissolution gases (nitrogen oxides) and the catalyst were found. The kinetics of this reaction was estimated from the experimental results. A model was then developed to describe and simulate these phenomena: it takes into account species transport between the particles surface and the bulk media, UO<sub>2</sub> dissolution kinetics, the reaction between the dissolution gases and the catalyst, as well as the transport of these gases to the liquid-gas interface. It was shown to be in good agreement with experimental results, at both microscopic and macroscopic scales. Dissolution modelling has now to be upgraded by integrating fragmentation and bubbling models.

## 1. Introduction

In France, the reprocessing of spent nuclear fuel is based on the liquid-liquid extraction of recoverable elements (uranium and plutonium) after its dissolution in nitric acid media. Dissolution is hence the key step of the head-end of the recycling process as it impacts the design of all the equipment of the industrial process. This study focuses on uranium dioxide as it accounts for about 96% of the spent fuel mass.

### 1.1 Description of uranium dioxide dissolution

Nitric dissolution of uranium is a complex reaction as it occurs in a heterogeneous liquid-solid medium, and couples chemical and hydrodynamic phenomena at different scales. The phenomena involved during this operation are illustrated in Figure 1. On the one hand, the reaction seems to be autocatalysed which means that the accumulation of the catalyst on the particles surface enhances dissolution (Marc (2014), Marc *et al.* (2018)). On the other hand, many parallel and/or consecutive reactions occur in the nitric medium and the dissolution reaction products are not all clearly identified (Sicsic *et al.* (2014), Schwartz and White (1983)). Thus, the nature of the catalyst (called Z in this study) itself is undefined. Moreover some reaction products are gaseous (NO and NO<sub>2</sub>) which makes uranium dissolution a triphasic reaction, with a phenomenon of bubbling which can sometimes be observed on the solid surface. Finally, previous studies have also shown the existence of preferential sites of attack, such as faults or grain boundaries, which also highlights the great

impact of the microstructure of the solid on dissolution kinetics. Thus, the complexity of dissolution relies both on the variety of phenomena and mechanisms, and their strong coupling illustrated in Figure 1.

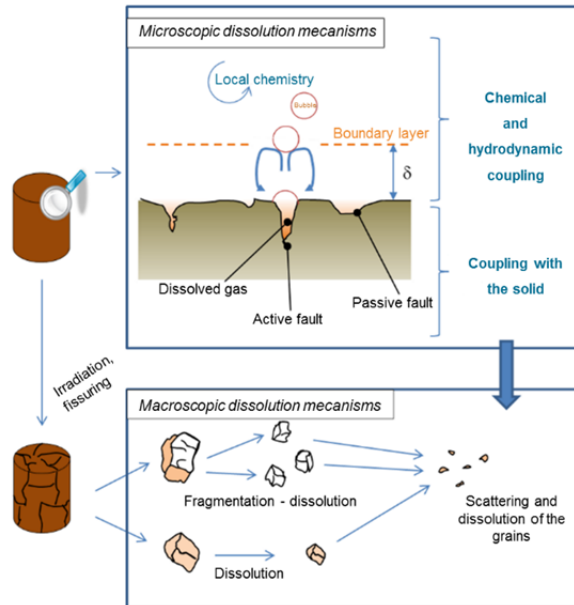


Figure 1: Description of mechanisms involved in the dissolution of nuclear fuel pellets

## 1.2 Aim of modelling

Eventually the objective is to have a dissolution model for various applications such as making optimisation solutions arising for the existing nuclear fuel dissolution reactors, but also for other processes involving autocatalysed and heterogeneous reactions. In addition, it would be a tool to test innovative configurations for the development of reactors for future reprocessing plants. Nevertheless, the construction of such a model requires a thorough understanding of the phenomena involved at different scales and the formalization of the dissolution kinetic rates.

## 2. Microscopic modelling of $UO_2$ particles dissolution

### 2.1 A microscopic model

A dissolution model was elaborated for single particles on the basis of a chemical-engineering approach by integrating the influence of hydrodynamics on heat and mass transfers, to determine the dissolution kinetic rates from the experiments described in section 2.2 at microscopic scale. The influence of mass transfer has a large impact on solid-liquid reactions, especially for autocatalysed reactions as the accumulation of the catalyst in the boundary layer considerably enhances kinetics. A model, taking into account the diffusion of the species and the peculiarities of the autocatalytic reaction, has been then elaborated. It includes the following elements (see Figure 2):

- the autocatalytic aspect of the reaction,
- the diffusion of species at both solid/liquid and liquid/gas interfaces,
- a volume reaction between catalyst and gas (in a first step, it was considered a reaction of the first order with respect to the reagents, reversible and independent from the concentration of nitric acid).

Modelling of bubbling is on progress and has not been implemented yet. The overall dissolution rate is represented in Eq(1) to Eq(3) as the sum of two parallel reactions: an uncatalysed reaction (subscripted nc) in which the catalyst Z has no influence, and a catalysed reaction (subscripted c).

$$r_{diss} = k_{nc}[HNO_3]^{n_1} + k_c[HNO_3]^{n_2}[Z]^p \quad (1)$$

$$k_{nc} = A_{nc} \exp\left(-\frac{E_{a_{nc}}}{RT}\right) \quad (2)$$

$$k_c = A_c \exp\left(-\frac{E_{a_c}}{RT}\right) \quad (3)$$

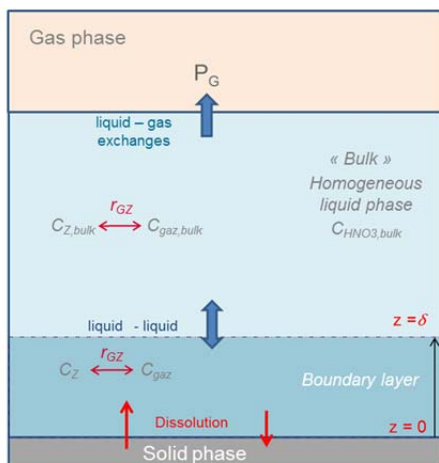


Figure 2: Description of the dissolution model –  $C_{i,bulk}$  = concentration of species  $i$  in the bulk –  $r_{GS}$  = volumic reaction between the catalyst  $Z$  and the gas products

## 2.2 Experimental setup

Dissolution rates are measured following the dissolution of oxide particles by observing their projected areas by optical microscopy (ZEISS Axio Vert.A1 Inverted Microscope). Image processing is done thanks to a homemade software developed on Scilab to extract areas and perimeters over time (see Figure 3). Indeed this method makes it possible to work with small particles, which improves liquid-solid mass transfer. In addition, a high liquid/solid ratio can be reached while limiting the production of effluents. Eventually, this enables working in situ without interfering with the reaction medium. The dissolving cell of 5 mL is equipped with a quartz base (Anacrismat) to observe particles without deformation, and a specific plug allowing the circulation of nitric acid. The method to extract kinetic rates from experimental data is detailed in the work of Charlier *et al.* (2017). Experiments were carried out both in catalysed and non-catalysed conditions to identify the two terms of the kinetic dissolution rate detailed in section 2.3.

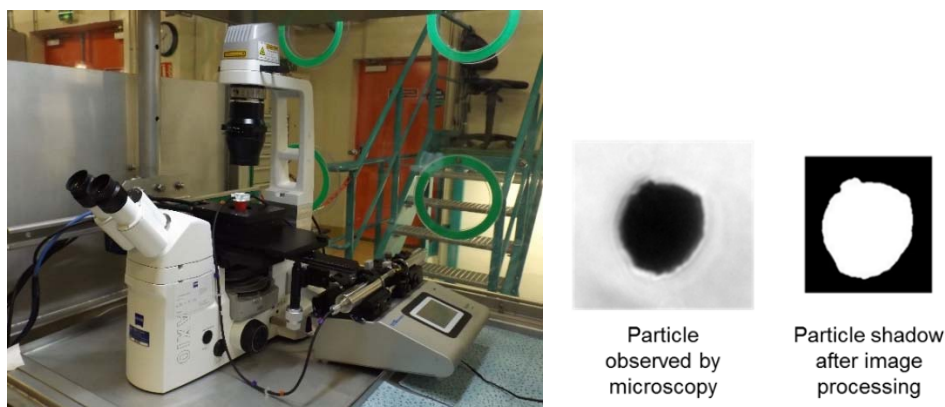


Figure 3: Experimental setup (left) and example of image processing of a dissolving particle (right)

## 2.3 Experimental results

The kinetic orders of the reaction relative to nitric acid and catalyst ( $n_1$ ,  $n_2$ ,  $p$ ) and activation energies parameters ( $A_{nc}$ ,  $E_{a_{nc}}$ ,  $A_c$  and  $E_{a_c}$ ) were determined from the comparison between the microscopic model described in section 2.1 and dissolution experiments carried out in different concentrations conditions and in the temperature range [30°C-70°C]. Values are detailed in Table 1.

Experimental results showed that catalyst loaded solutions tended to lose responsiveness over time. The influence of the gaseous products has therefore been suspected and their impact on the dissolution kinetics studied: the greater the liquid-gas exchanges, the faster the dissolution kinetics decrease over time. In addition, the reaction is accelerated when additional NOX gases are circulated in the dissolution

solution. It confirms the results of Nishimura *et al.* (1995) and Fukasawa *et al.* (1991) about a relationship between the catalyst of this dissolution and nitrogen oxides.

Table 1: dissolution kinetic parameters for uranium dioxide

|                   | Units  | Uncatalysed reaction                                  | Catalysed   |
|-------------------|--|---|---|
| Reaction orders   | -  | $n_1 = 3.5$   | $n_2 = 3.1 \pm 0.32$<br>$p = 0.75 \pm 0.15$       |
| Activation energy | $\text{kJ}\cdot\text{mol}^{-1}$                          | $E_{a_{nc}} = 62.7 \pm 3.7$                           | $E_{a_c} = 70.8 \pm 4.4$                          |
| Frequency factors | $\text{mol}^{1-x}\cdot\text{m}^{3y-2}\cdot\text{s}^{-1}$ | $A_{nc} = 1.2 \times 10^{-8} \pm 0.15 \times 10^{-8}$ | $A_c = 2.5 \times 10^{-4} \pm 1.0 \times 10^{-4}$ |

Application of the model shows that, with the assumptions applied, a scenario where the catalyst is produced from the gaseous dissolution products (and not the opposite) leads to a good description of experimental data: Figure 4 illustrates the evolution of the concentrations and the radius of three particles (initial radius: 8.3, 9.4 and 15 microns) dissolving in the same acidity and temperature conditions. In the first beginning of the experiment (red area), gaseous products accumulate in the boundary layer, which enhances the kinetics of the catalyst/gas reaction: accumulation of catalyst Z in the boundary layer is then promoted. As soon as the catalyst concentration is locally high enough, the size of the particles starts to decrease and mass transfer becomes faster, which, in a second step, leads to a slump in the Z accumulation and slowdown the catalysed dissolution reaction (blue area). At the end of the experiment (green area), dissolution is thus controlled by chemistry. The catalyst Z is not generated anymore and only the uncatalysed reaction, which is much slower than the catalysed one, takes place.

Eventually, the model and the associated assumptions describe successfully experimental data for the three sizes of particles. However they cannot describe the latency time which is experimentally observed at the first beginning of the dissolution (before red area). Investigation on gas solubility modelling is ongoing.

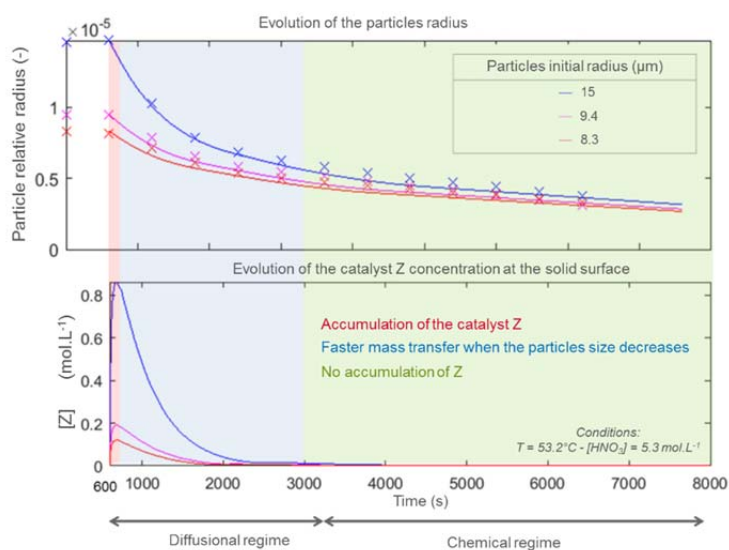


Figure 4: Comparison between experimental and simulated data

### 3. Macroscopic models for $\text{UO}_2$ powders

#### 3.1 Definition of the macroscopic model

A macroscopic model has been simultaneously developed to simulate  $\text{UO}_2$  powder dissolutions at higher scale (250 mL). It takes into account the dissolution reaction through the catalysed and uncatalysed terms determined at microscopic scale and evolution of particles size is described thanks to a population balance. Influence of hydrodynamics on the boundary layer surrounding particles and on mass transfer is defined through classical adimensional numbers (Reynolds, Schmidt and Sherwood) to allow a future scale up (to pilot or industrial scale). The final macroscopic model was compared with dissolution experiments carried out firstly in batch and semi-continuous perfectly mixed reactors to converge progressively towards a continuous type reactor. An example of a semi-batch dissolution is described in the following section.

### 3.2 Macroscopic dissolution set-up

Experiments were carried out with a  $\text{UO}_2$  powder initially characterized to qualify the model. They consist in initially introducing the powder in the dissolution reactor (see Figure 5) and to apply a continuous nitric acid feed. The dissolution state of advancement is followed by continuously monitoring the uranium concentration by spectrophotometry, and the acidity by taking regular samples.

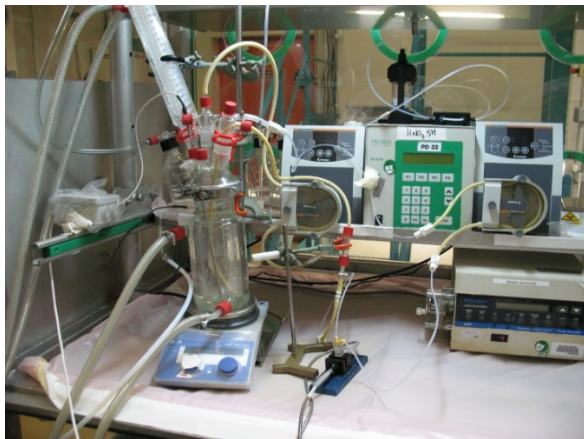


Figure 5: Experimental set-up to validate the macroscopic model

Experimental data are illustrated in Figure 6 for a dissolution of  $\text{UO}_2$  carried out at an initial acidity of 2N and an initial temperature of  $43^\circ\text{C}$ . Figure 6 shows the evolution of both uranium concentration (red dots) and acidity (blue dots). Direct application of the macroscopic model has pointed out that the kinetic parameters determined at microscopic scale do not lead to a good fit with experimental data (these results are not illustrated in the present work). However, after optimizing parameters, the model is in a good agreement with experimental data. Relative orders to nitric acid ( $n_1$  and  $n_2$ ) and catalyst Z ( $p$ ) were readjusted from macroscopic experiments and now give satisfactory results as illustrated in Figure 6 (red continuous line representing the simulated concentration of dissolved uranium). Indeed, not only is the model able to describe the concentration profiles but it is also able to follow the dynamics of the experiment as it simulates the impact of process perturbations (malfunction of the nitric acid feed) on the concentration profiles. However, as previously pointed out at microscopic scale, a latency time is still observed at the very first beginning of the experiment and cannot be simulated by the model. Thus, the initial modelling results are very encouraging but a better description of liquid-gas equilibria in boundary layers is still investigated to solve this problem. Optimised kinetic parameters are not given in this study as they will most likely be re-evaluated on that occasion.

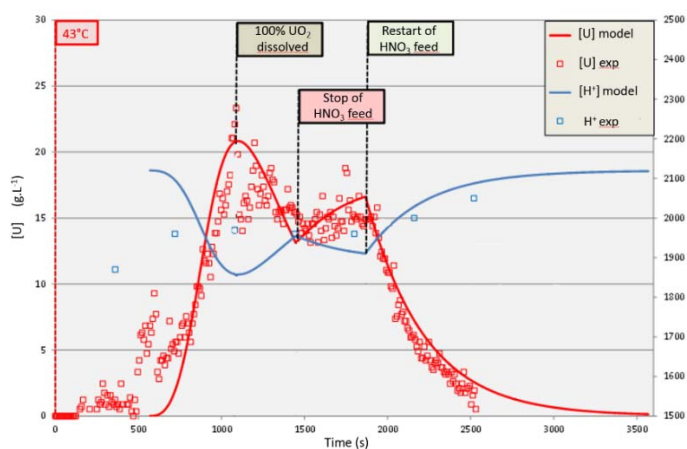


Figure 6: Evolution of uranium and acid concentrations during a semi-batch dissolution of  $\text{UO}_2$  powder –  $[\text{HNO}_3]_{\text{feed,ini}} = 2\text{N} - T_{\text{ini}} = 43^\circ\text{C}$

#### 4. What about pellets dissolution?

As illustrated in the previous section, the model developed initially for powders gives encouraging results. It has now to be upgraded to be applied to pellets and to take into account their fragmentation during dissolution. One of the currently developed models is based on the description of the solid as a staking of  $\text{UO}_2$  grains bonded together by a "cement" material which dissolves faster than grains and gradually releases them in the liquid (see Figure 7). This implies to consider different dissolution rates and a population balance reflecting the evolution of the grains sizes during their dissolution. Moreover, despite its great complexity, bubbling in the solid faults must be considered as it locally strongly impacts the mass transfer and thus the dissolution kinetics. Models are investigated to include this mechanism.

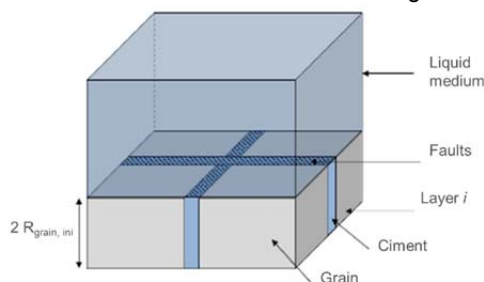


Figure 7: Illustration of the fragmentation model

#### 5. Conclusions

Experiments have pointed out that mass transfers are decisive at both liquid-solid and solid-gas interfaces and control the concentration of catalyst around the solid. Gas-liquid exchanges may then be a lever to control and optimise the catalyst accumulation to reduce the residence time of solid in dissolvers. Providing a slight correction of kinetic parameters from micro- to macroscopic scale, modelling gives encouraging results for both experimental scale. Efforts are now focused on modelling experimental latency times, bubbling and solid fragmentation.

#### Acknowledgments

Authors want to thank Orano and EDF for their financial support.

#### References

- Charlier F., 2017, Réactions autocatalytiques hétérogènes. Vers le dimensionnement de réacteurs de dissolution du dioxyde d'uranium, PhD thesis, Université de Lorraine
- Charlier F., Canion D., Gravinese A., Magnaldo A., Lalleman S., Borda G. and Schaer E., 2017, Formalization of the kinetics for autocatalytic dissolution. Focus on the dissolution of uranium dioxide in nitric acid, EPJ Nuclear Sci. Technol. 3, 26
- Fukasawa T., Ozawa Y. and Kawamura F., 1991, Generation and decomposition behaviour of nitrous acid during dissolution of  $\text{UO}_2$  pellets by nitric acid, J. Nucl. Technol. 91
- Marc P., Magnaldo A., Godard J. and Schaer E., 2018, A method for phenomenological and chemical kinetics study of autocatalytic reactive dissolution by optical microscopy. The case of uranium dioxide dissolution in nitric acid media, EPJ Nuclear Sci. Technol. 4, 2
- Marc P., 2014, Etude de réactions hétérogènes autocatalytiques. Application à la dissolution du dioxyde d'uranium, PhD thesis, Université de Lorraine
- Nishimura K., Chikasawa T., Hasegawa S. and Tanaka H., 1995, Effect of nitrous acid on dissolution of  $\text{UO}_2$  powders in nitric acid. Optimal conditions for dissolving  $\text{UO}_2$ , J. Nuclear Sci. Technol. 32, 157
- Sicsic D., Balbaud-Celerier F. and Tribollet B., 2014, Mechanism of nitric acid reduction and kinetic modelling, Eur. J. Inorg. Chem. 2014, 6174-6184
- Schwartz S.E. and White, W.H., 1983, Kinetic of reactive dissolution of nitrogen into aqueous solution, Adv. Environ. Sci. Technol. 12